

RealVVT: Towards Photorealistic Video Virtual Try-on via Spatio-Temporal Consistency

Siqi Li¹ Zhengkai Jiang² Jiawei Zhou³ Zhihong Liu⁴ Xiaowei Chi² Haoqian Wang^{3†}

¹Intellifusion ²HKUST ³THU ⁴FDU

tristanafourseven@gmail.com wanghaoqian@tsinghua.edu.cn

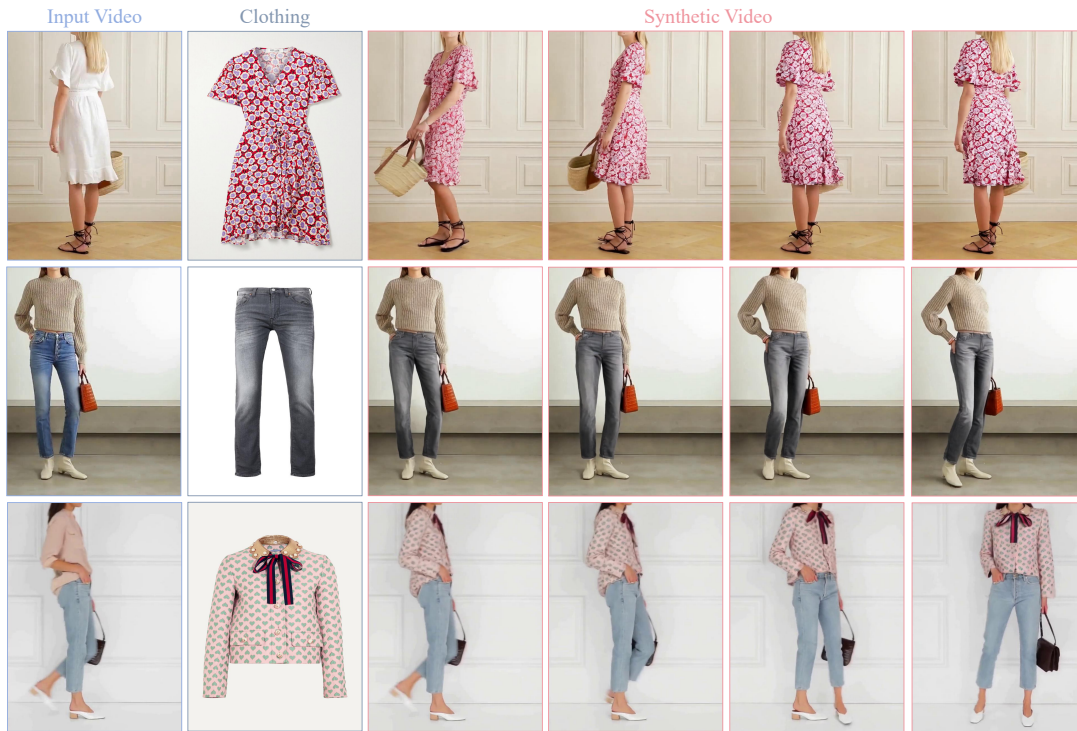


Figure 1. Generated results of RealVVT. Our model achieves state-of-the-art performance in video try-on tasks, maintaining remarkable spatial and temporal consistency on dresses, lower body, and upper body garments try-on tasks, regardless of human pose variations.

Abstract

Virtual try-on has emerged as a pivotal task at the intersection of computer vision and fashion, aimed at digitally simulating how clothing items fit on the human body. Despite notable progress in single-image virtual try-on (VTO), current methodologies often struggle to preserve a consistent and authentic appearance of clothing across extended video sequences. This challenge arises from the complexities of capturing dynamic human pose and maintaining target clothing characteristics. We leverage pre-existing video

foundation models to introduce RealVVT, a photoRealistic Video Virtual Try-on framework tailored to bolster stability and realism within dynamic video contexts. Our methodology encompasses a Clothing & Temporal Consistency strategy, an Agnostic-guided Attention Focus Loss mechanism to ensure spatial consistency, and a Pose-guided Long Video VTO technique adept at handling extended video sequences. Extensive experiments across various datasets confirms that our approach outperforms existing state-of-the-art models in both single-image and video VTO tasks, offering a viable solution for practical applications within the realms of fashion e-commerce and virtual fitting environments.

[†]Corresponding authors.

1. Introduction

With advancements in image-based virtual try-on (VTO) technology, the demand for video virtual try-on (VVT) has grown significantly, driven by the need to capture and display the dynamic appearance of clothing on a target individual across video sequences. VVT not only preserves the garment’s details but also ensures that clothing aligns naturally with the person’s motions and body shapes, offering users an immersive experience to visualize how desired clothing fits and moves from various angles. This innovation has garnered substantial attention for two main reasons: first, its practical applications in the fashion industry and entertainment, and second, its potential to inspire new directions for video editing tasks based on image prompts, both of which have accelerated developments in this field.

The task of video virtual try-on (VVT) presents significant challenges, as it extends beyond static operations such as mapping a garment to a predefined mask. Unlike static images, VVT must account for dynamic human poses and varying viewpoints, which complicates the accurate fitting of clothing to the target individual. The movement of the person and changes in perspective can distort the appearance of the clothing, making it difficult to maintain the garment’s shape, style, and texture. Furthermore, ensuring spatial and temporal consistency of the clothing throughout a video sequence plays a critical role in the success of VVT. Previous approaches [15, 21, 22] have used optical flow estimation and completion techniques to address this problem, where the garment is warped using optical flow and misalignments are corrected through additional generative mechanisms such as GANs [22] or Transformers [15]. More recently, diffusion-based methods [13, 14, 37, 41] have emerged, adapting text-to-image virtual try-on techniques to the video domain. These methods [14, 37, 41], which integrate temporal modules or consistency constraints, offer promising avenues for VVT. Additionally, some approaches [13] have directly adapted text-to-video diffusion models for VVT, demonstrating the potential of modeling the transformation of garments according to the different poses and motions of the target individual. However, video virtual try-on still faces three primary challenges: **Temporal Inconsistency**: Maintaining consistent clothing appearance as the wearer moves remains a major hurdle. Existing methods often generate video sequences where the clothing appears flickering or unstable. **Spatial Inconsistency**: The garment often adheres to the shape and color of the target mask, making it difficult to retain the original garment’s shape, style, and texture. **Long Video Inaccuracy**: Sequential frame-by-frame generation tends to accumulate errors over time, especially when dealing with complex body movements and occlusions. As a result, some frames may exhibit unexpected outcomes, leading to cumulative inconsistencies.

To address the aforementioned three challenges, we introduce a novel approach, RealVVT (Realistic Video Virtual Try-on), that effectively addresses these challenges by harnessing the capabilities of diffusion models, which have recently demonstrated exceptional performance in both image and video generation tasks. Our framework is grounded in Stable Video Diffusion (SVD) [1], a robust image-to-video architecture, and is enhanced with several key innovations designed to ensure high-quality and temporally coherent virtual try-on results.

To enhance video generation quality, we focus on improving both spatial and temporal consistency. Regarding Spatial Consistency, we introduce the **Agnostic Mask-Guided Attention Loss** to ensure accurate intra-frame garment fitting. This loss function directs the model to prioritize the areas where the garment should be worn, while reducing attention to background and non-wearable body regions. This enables better preservation of the garment’s shape, style, and texture. Additionally, the model fills mask regions beyond the garment appropriately, ensuring spatial alignment and maintaining the garment’s authentic appearance across the generated sequence, resulting in a more coherent and realistic video output. For temporal consistency, we propose a **Clothing & Temporal Consistency Attention mechanism** to ensure inter-frame coherence. By leveraging the interactive information between the two U-Nets [6], this mechanism tightly integrates reference and temporal information, enforcing temporal coherence and ensuring that the clothing remains stable and aligned with the wearer’s body, even with pose changes or camera shifts. This approach significantly reduces flickering and misalignment, contributing to a more immersive and realistic virtual try-on experience. To address inaccuracies in long video sequences, we introduce the **Pose-guided Long VVT strategy**, which effectively utilizes pose inputs to estimate motion and viewpoint changes. By iteratively generating long videos through keyframe replacement, this strategy preserves motion realism and clothing coherence throughout the entire sequence. Experiments on several high-quality image and video datasets demonstrate the superior performance in both short- and long-video virtual try-on tasks. Fig. 1 illustrates our generated results. In summary, the contributions of this paper are threefold:

- Agnostic Mask-Guided Attention Loss focusing on the garment-wearing areas and minimizing attention to non-wearable regions.
- Clothing & Temporal Consistency Attention Mechanism integrating reference and temporal information across frames, reducing flickering and misalignment.
- Pose-guided Long VVT strategy for long video sequences, preserving motion realism and garment coherence by iteratively video generation.

2. Related Work

2.1. Video Virtual Try-On

Video try-on aims to transfer a garment onto a target individual while preserving the garment’s shape and visual details over time as the person moves or changes perspective. Existing approaches to video virtual try-on can be broadly categorized into GAN-based [15, 20–22] and diffusion-based methods [14]. GAN-based methods typically depend on optical flow to warp the garment [19] and employ a GAN generator to blend the warped garment with the person. GAN-based models are sensitive to misalignment between the garment and the person due to inaccurate flow estimations and often lag behind diffusion-based models in generation quality due to the latter’s use of large-scale pretrained weights. The era of diffusion has arrived, Tunnel Try-on [14] employs a UNet-based model for video try-on, enabling it to handle camera movements and accurately preserve clothing textures. ViViD [41] introduced a high-resolution dataset (832×624) for video try-on, addressing the limitation of prior datasets like VVT [4], which offered only low-resolution samples. VITON-DiT [13] generates try-on sequences in-the-wild settings by using the DiT structure [18]. However, its text-to-video architecture is redundancy and inefficient. Meanwhile, WildVidFit [37] employs a two-stage, image-generation-based framework for try-on, trained in two separate stages and lacking the abilities of temporal coherence and preserving fine details. Building upon these prior approaches, we introduce RealVVT, a one-stage training framework for video try-on that achieves high-quality synthesis with superior spatio-temporal consistency, and maintaining efficiency.

2.2. Video Generation via Diffusion Models

With continued advancements in diffusion-based image synthesis techniques [9, 29, 30], numerous frameworks have been developed to extend diffusion models for video synthesis. Some approaches train video diffusion models from scratch by incorporating temporal layers [27, 28], while a more prevalent strategy involves adapting pretrained image diffusion models for video by adding temporal layers and fine-tuning them specifically for video generation tasks [10, 11, 26]. However, these approaches still face challenges struggle with maintaining fine-grained texture consistency and temporal coherence across frames, especially when complex garment details need to be preserved throughout varying poses and movements in a video sequence. The DiT structures [23–25] can effectively capture spatio-temporal dependencies, their computational demands increase significantly with higher resolutions and longer sequences, posing challenges for high-fidelity video try-on applications. SVD [1] exemplifies this approach: it builds upon a latent image diffusion model [12] and is

adapted to video synthesis with additional temporal components, including 3D convolutions and temporal attention layers. SVD is well-suited for maintaining high levels of spatial and temporal coherence, as it leverages pretrained image diffusion capabilities while incorporating temporal modeling to ensure frame-to-frame consistency. Building on the large-scale pretrained SVD model, we introduce a new method that achieves significantly enhanced spatial and temporal consistency compared to prior models.

3. Proposed Approach

We first review some foundational concepts of video diffusion models in Sec. 3.1. Following this, Sec. 3.2 offers a detailed overview of the overall network architecture of our RealVVTmodel. In Sec. 3.3, we introduce an Agnostic-guided Attention Focus Loss, which can improve spatial consistency. Subsequently, in Sec. 3.4, we describe our method to achieve temporal consistency. Finally, we present a pose-guided strategy in Sec. 3.5 for long video virtual try-on generation.

3.1. Preliminary

Our primary UNet backbone leverages Stable Video Diffusion [1] model to jointly train videos and images in a unified framework, utilizing the EDM [2] diffusion model with Euler-step sampling strategy.

Video Diffusion Model. Stable Video Diffusion (SVD) was initially developed for the purpose of video generation, leveraging a single image as the initial frame. This model consists of a Variational Autoencoder (VAE) [3] and a UNet architecture that incorporates spatio-temporal blocks. The VAE encoder transforms input video frames into a lower-dimensional latent space, while the decoder reconstructs these latent representations back into the frame space. To mitigate temporal inconsistencies and reduce flickering artifacts, temporal layers are integrated within the VAE. In the latent space, a conditional spatio-temporal U-Net is employed for denoising, utilizing both spatial and temporal information through 3D convolutional layers. This architecture effectively integrates conditional inputs to enhance the denoising process.

EDM. In Stable Video Diffusion (SVD), the denoiser D_θ receives the clean image from the outputs of the UNet U_θ :

$$D_\theta(x; \sigma, c) = c_{skip}(\sigma) \cdot x + c_{out}(\sigma) \cdot U_\theta(c_{in}(\sigma) \cdot x; c_{noise}(\sigma), c) \quad (1)$$

where σ denotes the noise level of the distribution, while $c_{skip}(\sigma)$, $c_{out}(\sigma)$, $c_{in}(\sigma)$, and $c_{noise}(\sigma)$ are EDM preconditioning parameters that depend on the noise level. The variable c represents the conditional input (e.g., the first frame in SVD and cloth information in our approach). As a training loss, SVD employs a continuous-time diffusion

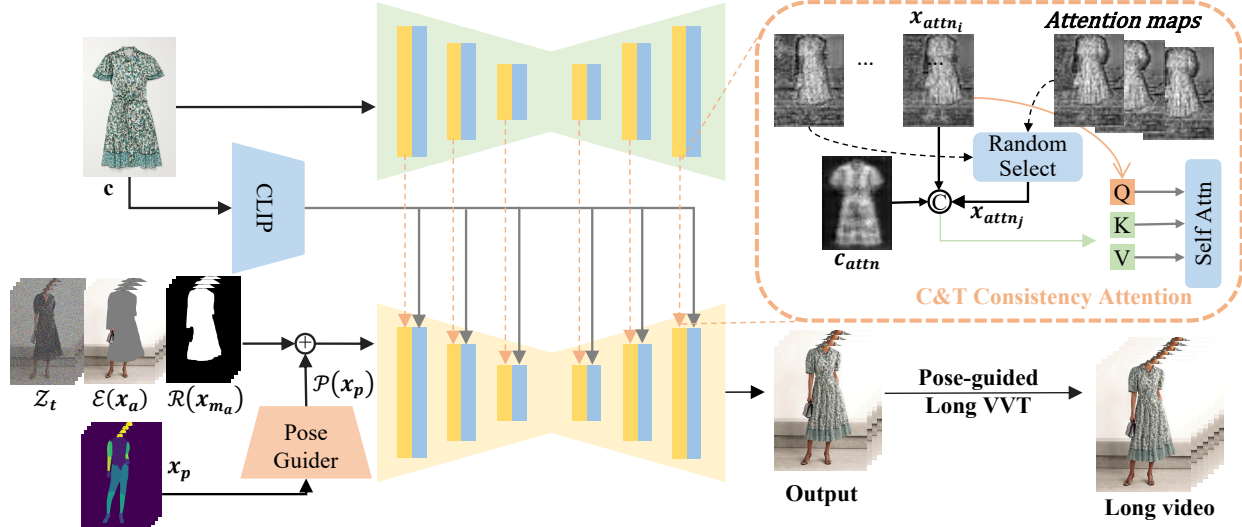


Figure 2. An overview of RealVVT. A Reference U-Net and CLIP Encoder extract garment features, while the input video is processed by a Spatial-Temporal U-Net. The right side illustrates the mechanisms of Clothing & Temporal Consistency Attention and Pose-guided Long VVT components. In C&T Consistency Attention, the feature of the current frame (x_{attn_i}), another feature from a random selected frame (x_{attn_j}), and the corresponding clothing feature from the Reference U-Net (c_{attn}) are concatenated as the key and value in self attention.

framework, EDM, in conjunction with the Denoising Score-Matching (DSM) loss function to train the denoiser D_θ :

$$\mathbb{E}_{(x_0, c) \sim p_{\text{data}}, (\sigma, n) \sim p(\sigma, n)} \left[\lambda_\sigma \|D_\theta(x_0 + n; \sigma, c) - x_0\|_2^2 \right] \quad (2)$$

Here, $p(\sigma, n)$ represents the distribution of the noise level σ and normal noise n , while λ_σ denotes the loss weights across different noise levels.

3.2. Overview

Overall Architecture. This section delineates the overall architecture of the pipeline, as depicted in Fig. 2. The foundation of RealVVT is constituted by two U-Nets: the Spatial-Temporal U-Net and the Reference U-Net [6]. The Spatial-Temporal U-Net is primarily tasked with the denoising of videos and is initialized with an image-to-video SVD model. The Reference U-Net has demonstrated efficacy in retaining the nuanced details of reference images. Consequently, we employ the Reference U-Net to encode the intricate features of the reference cloth image $c \in \mathbb{R}^{H \times W \times 3}$, which is the garment we intend to virtually drape, and leverages the Spatial-Temporal U-Net to process the person video data.

Video Virtual Tryon Preprocess. Consider a person video $x \in \mathbb{R}^{N \times H \times W \times 3}$, where N signifies the frame count during the training phase. We introduce the Clothing-Agnostic Person Representation $x_a \in \mathbb{R}^{N \times H \times W \times 3}$ [35], termed the agnostic video, which is crafted to eradicate all vestiges of the attire we aspire to substitute within x . In this endeavor, we conceptualize the video virtual try-on task as an exemplar-based video inpainting challenge, aiming to re-

plenish the agnostic mask region in the agnostic video x_a with the cloth c and to leverage the unmasked regions in x_a for providing more granular details about the individual (e.g. skin tone). For the U-Net’s input, we amalgamate three constituents: (1) the noisy frames (Z_t , 4 channels); (2) the latent agnostic video frames ($\mathcal{E}(x_a)$, 4 channels); and (3) the resized cloth agnostic masks ($\mathcal{R}(x_{m_a})$, 1 channel, F frames) to delineate the inpainting zone and to set the stage for the Agnostic-guided Attention Focus Loss. To harmonize the input channels, we augment the initial convolutional layer of the U-Net to accommodate 9 channels (i.e., $4+4+1=9$) via a convolutional layer. Thereafter, the model assimilates dense pose ($\mathcal{P}(x_p)$) from the pose estimator, which is instrumental in ensuring that the denoising process maintains the motion and posture of the individual.

3.3. Agnostic Mask-Guided Attention for Clothing Consistency

In attention mechanism, the attention probability scores, denoted as T , represents the attention weight distribution across different regions, with higher values indicating areas where the model allocates more focus. Given the objective of replacing the original clothing with the target garment, we aim to ensure that the regions covered by the agnostic mask—indicating the areas to be replaced—receive increased attention on the target garment. To achieve this, we introduce a novel loss function specifically designed to enhance attention efficacy in the agnostic mask region. The initial formulation is as follows:

$$\mathcal{L}_{\text{agn-init}} = \sum_{i \in N} \sum_{a \in A} (1 - T_i^a)^2 + \lambda_N \sum_{i \in N} \sum_{a \in \bar{A}} \|T_i^a\|^2, \quad (3)$$

where N represents the length of the video sequence, A represents the region defined by the agnostic mask, and \bar{A} denotes its complement, then T_i^a denotes the attention probability for the target garment at location a in frame i . This loss encourages attention probabilities within the agnostic mask region to focus on the target garment, while suppressing attention in non-mask regions. The parameter λ_N controls the balance between positive and negative attention contributions.

However, our goal is not merely to fill the mask region with the target garment, but rather to replace clothing A with clothing B, which may differ in shape, style, or coverage. In practice, it is uncommon for the agnostic mask to perfectly align with the structure of the target garment, particularly when the replacement involves significant style differences (e.g., swapping pants for shorts or a short-sleeve shirt for a long coat). In such scenarios, determining the proper placement of clothing B within the mask region is crucial. Additionally, the model must appropriately fill the regions outside B and inside agnostic mask with contextual information, such as skin tone or limb shape, to infer the appearance of occluded body parts.

To address these complexities, we modify the loss function to enhance attention in the most relevant regions, rather than uniformly distributing attention across the entire mask, guiding the model to focus on areas with a high attention probability. Our revised loss function is defined as:

$$\mathcal{L}_{\text{agn}} = \sum_{i \in N} (1 - \max_{a \in A} T_i^a)^2 + \lambda_N \sum_{i \in N} \sum_{a \in \bar{A}} \|T_i^a\|^2. \quad (4)$$

This approach strengthens the model’s ability to infer context beyond the strict boundaries of the agnostic mask, thereby better preserving the original characteristics of the clothing. Finally, we finetune our RealVVT by adding \mathcal{L}_{agn} to $\mathbb{E}_{(x_0, c)}$:

$$\mathcal{L}_{\text{modified}} = \mathbb{E}_{(x_0, c)} + \lambda_{\text{agn}} \mathcal{L}_{\text{agn}}. \quad (5)$$

The parameter λ_{agn} controls the inference of agnostic mask-guided loss impacting on the total loss.

3.4. Clothing&Temporal Consistency Attention

Fig. 3(a) and (b) highlight the limitations of current virtual try-on methodologies. While these approaches effectively generate clothing that adapts to the video’s progression, they often struggle to maintain temporal consistency and generate the clothing flickering or flowing, with textures that shift independently of the wearer’s motion. To

address this issue, we introduce the Clothing & Temporal Consistency Attention mechanism, which enhances both the fidelity of the clothing and the temporal coherence of the sequence.

To achieve this, it is imperative to establish inter-frame connections within the video sequence while ensuring consistency with the target clothing during the generation process. A re-evaluation of existing attention mechanisms within diffusion models has prompted us to investigate self-attention as a means to guarantee consistency across video frames. In certain implementations, the keys and values, denoted as K and V , are constructed by concatenating all frames in the video, thereby facilitating attention across the entire sequence. However, this methodology is computationally demanding and necessitates substantial memory resources. To address this challenge, the cross-frame attention mechanism typically utilizes only the initial frame and the preceding frame as references. Specifically, cross-frame attention is generally defined as:

$$V_i = \text{Softmax} \left(\frac{Q_i K_{p_i}^T}{\sqrt{d}} \right) V_{p_i} \quad (6)$$

where Q_i , K_{p_i} , and V_{p_i} are the query, key, and value matrices for frame i , d is the dimension of the key vectors, p_i is the cross-frame index. Since the same operation is applied to both K and V , we use x_{attn} to represent the unified operation on K and V for brevity. The following describes the basic operation of cross-frame attention:

$$X_{\text{attn}_{p_i}} = \text{Concat}(X_{\text{attn}_0}, X_{\text{attn}_{i-1}}) \quad (7)$$

In contrast to autoregressive models that generate video frames sequentially in temporal order, our approach emphasizes maintaining the temporal consistency of clothing appearance across varying angles and actions of the individual wearing the same garment. Consequently, random actions or viewpoints are more important than the temporal order in ensuring consistency. We enhance this by utilizing a randomly selected reference frame and the current frame i , which serves to fully leverage the available input information. This allows our method to effectively capture alignment information from both the present and distant frames, even if the garment image depicts a front view while the individual enters from a side or back view (e.g. Fig. 3).

Crucially, to uphold a consistent clothing appearance, we directly integrate the reference clothing features into the attention mechanism. Therefore, the key feature for frame i is defined as:

$$X_{\text{attn}_{p_i}} = \text{Concat}(X_{\text{attn}_i}, X_{\text{attn}_j}, c_{\text{attn}}) \quad (8)$$

where j denotes the index of a randomly selected frame and c_{attn} represents the features extracted from the reference clothing image.

By incorporating both temporal references and clothing-specific features into the attention mechanism, our approach significantly enhances temporal consistency, ensuring that the individual appears to wear the same clothing throughout the video sequence, irrespective of variations in perspective or motion.

Algorithm 1 Pose-guided Long VVT

Input: Agnostic video $\mathbf{A} = \{a_i\}_{i=1}^F$, Agnostic mask $\mathbf{M} = \{m_i\}_{i=1}^F$, DensePose frames $\mathbf{P} = \{p_i\}_{i=1}^F$, sample parameters d_{pose}, s_{max}

Output: Video sequences generated $\mathbf{V} = \{V_i\}_{i=1}^F$

Step 1: Keyframe Selection and Generation

Initialize keyframe index $\Omega = [0]$ and $i = 0, j = 1$ **while** $j < F$ **and do**

Compute L2 distance $\|p_i - p_j\|_2$

if $\|p_i - p_j\|_2 < d_{pose}$ **or** $|i - j| < s_{max}$ **then**

$\Omega.insert(i).sort(), i = j,$

do $j+ = 1$

Generate keyframes $\mathcal{V} = \{v_0, \dots, v_L\}$

Step 2: Keyframe Interpolation Replacement

Replace $v_i \mapsto a_i$ **if** $i \in \Omega$

Divide original $[\mathbf{A}, \mathbf{M}, \mathbf{P}]$ **into segments** $\{s_1, s_2, \dots, s_n\}$

Iteratively generate and concatenate to complete \mathbf{V}

3.5. Pose-guided Long VVT

Building upon enhanced spatial and temporal consistency, RealVVT can already produce high-quality, fixed-length video virtual try-on sequences of N frames. To extend this capability to longer video sequences, we adopt a zero-shot keyframe selection strategy inspired by video translation tasks (e.g., Rerender-A-Video [8]). We then interpolate the generated keyframe outputs, treating them as agnostic video frames, to iteratively produce the remaining try-on results.

Keyframes Selection. While Rerender-A-Video [8] adopts a uniform keyframe sampling approach, subsequent video generation methods [42, 43] improve upon this by sampling frames based on frame similarity, which may be suboptimal in the VVT task. The most significant factor is the magnitude of pose and motion changes, whereas variations in background or facial expressions can complicate the accurate estimation of motion magnitude. To address this, we utilize the L2 distance between DensePose frames as a measure of object motion. DensePose frames feature a clean, monochromatic background (RGB: 0, 0, 0) and use distinct color blocks to represent different body parts, minimizing the influence of facial or background changes. This eliminates the need for blurring techniques, such as Gaussian Blur, used in prior methods for long video generation to suppress high-frequency texture changes. By calculating the distances between DensePose frames, we select frames with distances below a threshold d_{dense} and strides under a

maximum s_{max} as input frames.

Keyframe Agnostic Replace. We store latent features of keyframe video outputs, and interpolate them back into the original agnostic video sequence, replacing the corresponding keyframe agnostic frames to iteratively complete the remaining generation. For sequences with keyframes exceeding N , the video is segmented into overlapping segments, where overlapping agnostic frames in subsequent segments are replaced with the denoised results from previous segments.

4. Experiments

Dataset. We conduct the experiments using two publicly available image virtual try-on datasets, VITON-HD [35] and DressCode [7], and two video datasets, ViViD [41], VVT [4]. VITON-HD is an image dataset focused on upper garment virtual try-on, containing high-resolution image pairs for garment swapping. DressCode, on the other hand, is a comprehensive and extensive high-resolution image dataset that includes a wide variety of clothing items, such as tops, lowerbodies, and dresses, for both men and women. Vivid, a newer video-image pair dataset, offers a resolution of 832×624 . To improve the stability of video generation results, we jointly train using both image datasets and high-resolution video datasets. For a fair evaluation against baselines, we used a model trained at a resolution of 512×384 . To assess the video editing performance of our method, we conducted evaluations on the VVT dataset on a uniform resolution of 512×384 pixels. Additionally, we evaluated our method on the VITON-HD and DressCode image dataset at the image original resolution of 1024×768 to demonstrate that our approach also performs well for image-based try-on tasks.

Furthermore, if these four datasets miss to provide any of the necessary inputs, such as agnostic video, agnostic mask, and densepose, we supplement them by using Detecron2 [44] and SAPIENS [5].

Implementation details. The experiment is conducted on eight NVIDIA Tesla A800 GPU. We set batch size = 2 based on the input video resolution, the learning rate is set to $5e^{-5}$. For the details in Eq. (4), the agnostic mask loss weight, λ_{agn} , is set to 0.5, and the scale factors, λ_N , is set to 0.01. λ_N determines the proportion of negative samples, calculated as the sum of all background tokens (out of mask), while the positive sample is only one token corresponding to the maximum value. Given a 19×12 feature map size corresponding to a training resolution of 512×384 , the number of negative tokens is approximately 120 times that of the single positive token. Therefore, λ_N is fixed at 0.01. The backbone we use is a combination of Reference U-Net and a Spatial-Temporal U-Net, pre-trained with Stable Diffusion 2.1 and Stable Video Diffusion XT respectively.

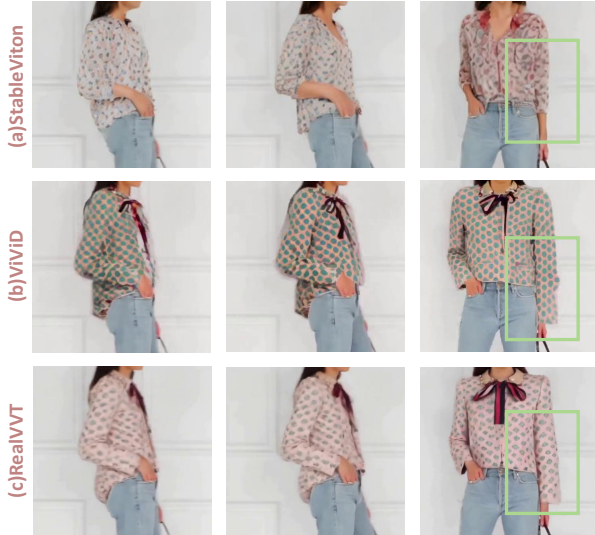


Figure 3. Virtual comparison with latest virtual try on method. The input garment, the original video and complete generated video sequence is shown in Fig. 1

Method	SSIM \uparrow	LPIPS \downarrow	VFID _{13D} \downarrow	VFID _{ResNeXt} \downarrow
ClothFormer [15]	0.921	0.081	3.97	5.05
StableVITON [17]	0.876	0.076	4.021	5.076
Tunnel Try-on [14]	0.913	<u>0.054</u>	3.345	4.614
VITON-Dit [13]	0.896	0.080	2.498	<u>0.187</u>
ViViD [41]	<u>0.949</u>	0.068	3.405	5.074
WildVidFit [37]	-	-	4.202	-
Ours	0.976	0.037	<u>2.689</u>	0.0913

Table 1. Quantitative comparison on the VVT dataset. **Bold** and underline denote the best and the second best result, respectively. The following tables are presented in the same way.

Method	SSIM \uparrow	LPIPS \downarrow	FID \downarrow	KID \downarrow
CP-VTON [31]	0.785	0.2871	48.86	4.42
HR-VTON [32]	0.878	0.0987	11.80	<u>0.37</u>
LaDI-VTON [33]	0.871	0.0941	13.01	0.66
DCI-VTON [34]	0.882	<u>0.0786</u>	11.91	0.51
WildVidFit [37]	<u>0.883</u>	0.0773	<u>8.67</u>	0.51
Ours	0.890	0.101	7.844	0.151

Table 2. Quantitative comparison on the VITON-HD dataset.

4.1. Comparison with State-of-the-Art Methods

Metrics. For quantitative evaluation, We evaluate our method on both a video dataset, vvt, and two image datasets, VITON-HD and Dresscode. Due to the lack of fair training results for other methods on the Vivid dataset, we only provide visual results for Vivid as proof of concept. We follow the video generation evaluation paradigm of vitondit by using SSIM, LPIPS, VFID_{13D} and VFID_{ResNeXt} scores. For image generation quality assessment, we use SSIM, LPIPS, FID and KID scores followed StableVITON. **Video Dataset Evaluation.** We compare our method with previous approaches on video datasets, visualizing results alongside ViViD(a video-based method), and Stable-



Figure 4. Virtual results of fitting a small garment onto a large agnostic mask video.

Method	SSIM \uparrow	LPIPS \downarrow	FID \downarrow	KID \downarrow
CP-VTON [31]	0.820	0.2764	57.70	4.56
HR-VTON [32]	0.924	0.0605	13.80	0.28
LaDI-VTON [33]	0.915	0.0620	16.71	0.61
GC-DM [38]	0.915	0.0649	14.91	6.01
WildVidFit [37]	<u>0.928</u>	0.0432	<u>12.48</u>	<u>0.19</u>
Ours	0.932	<u>0.0608</u>	8.881	0.163

Table 3. Quantitative comparison on DressCode-Upper dataset.

Method	SSIM \uparrow	LPIPS \downarrow	FID \downarrow	KID \downarrow
PBE [40]	0.804	0.2108	22.44	6.78
MGD [39]	0.893	0.0689	13.67	3.79
LaDI-VTON [33]	<u>0.910</u>	0.0596	13.76	4.61
GC-DM [38]	0.902	<u>0.0621</u>	<u>10.25</u>	<u>1.81</u>
Ours	0.912	0.0743	9.204	0.256

Table 4. Quantitative comparison on DressCode-Lower dataset.

Method	SSIM \uparrow	LPIPS \downarrow	FID \downarrow	KID \downarrow
PBE [40]	0.761	0.2516	30.04	18.44
MGD [39]	0.844	0.1195	12.14	2.41
LaDI-VTON [33]	0.854	<u>0.1076</u>	13.00	4.05
GC-DM [38]	<u>0.863</u>	0.1091	<u>10.71</u>	<u>2.02</u>
Ours	0.888	0.0932	10.45	0.239

Table 5. Quantitative comparison on DressCode-Dresses dataset.

VITON(an image-based method), in Fig. 3. Video results are more evident than a short three-frame sequence, clearly showing that methods like Fig. 3(a) exhibit significant flickering, while video-based methods like vivid greatly improve temporal coherence, shown in Fig. 3(b), eliminating flickering but still presenting the clothing flowing as if worn on a screen, as discussed in Sec. 3.4. Our approach achieves superior consistency in maintaining the color, shape, and fine details of the clothing. Fig. 4 demonstrates that the Agnostic Mask-Guided loss prevents the model from simply overlaying the clothing in the agnostic mask, ensuring accurate generation of the garment’s expected shape, and the comparisons with other methods are provided in the supplementary material. Additionally, we evaluate our method using standard video generation metrics on the VVT dataset in Tab. 1, where it outperforms prior methods generally. Notably, our

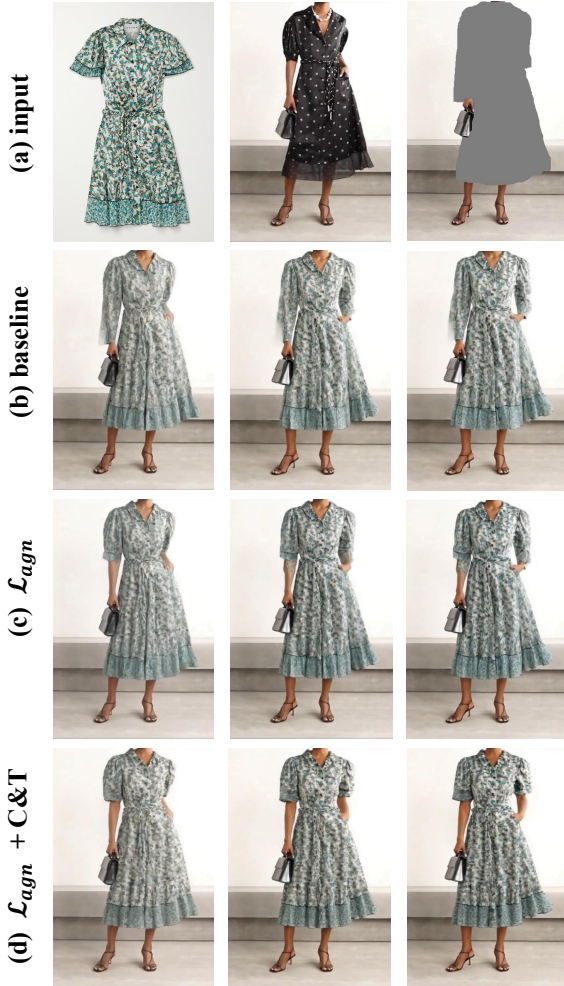


Figure 5. Effect of Agnostic Mask-Guided loss and Clothing & Temporal Consistency Attention. The first and third images in (a) are input frames, while the second image is not used as input and instead serves to illustrate the original video.

method shows significant improvements in SSIM, LPIPS, and VFID_{ResNeXt}, underscoring its effectiveness in producing temporally coherent and detail-preserving results.

Image Dataset Evaluation. We evaluated our model on four distinct datasets, including the VITON-HD test set and the DressCode test subsets (LowerBody, UpperBody, and Dresses). For these four datasets, we compared our method against the best-performing approaches available that provide these evaluation metrics in Tab. 2, Tab. 3, Tab. 4, and Tab. 5. Furthermore, our visual comparisons will be presented in the supplementary materials. Our results demonstrate a clear performance advantage across all datasets, affirming the robustness and adaptability of our approach in various virtual try-on scenarios.

4.2. Ablation Study

To demonstrate the effectiveness of RealVVT in addressing spatial and temporal consistency, we investigate the im-

C&T	λ_{agn}	SSIM \uparrow	LPIPS \downarrow	VFID _{I3D} \downarrow	VFID _{ResNeXt} \downarrow
-	0	0.890	0.145	6.119	0.522
-	0.05	0.901	0.150	6.102	0.531
-	0.1	0.905	0.102	5.278	0.235
-	0.5	0.910	0.096	4.761	0.151
+	0.5	0.976	0.037	2.689	0.0913

Table 6. Quantitative ablation study of λ_{agn} and C&T.

part of two proposed components during training: the Agnostic Mask-Guided loss (λ_{agn}), with a fixed λ_N of 0.1, and the Clothing & Temporal Consistency Attention mechanism (C&T). Fig. 4 show the visualization results. And Tab. 6 shows the quantitative performance improvements after adding these components. The first four rows in Tab. 6 present results without C&T, with each successive row indicating a larger λ_{agn} value. In the second row, with $\lambda_{agn} = 0.05$, the agnostic loss has minimal impact, resulting in stable metrics with no significant changes. The VFID_{I3D} value shows a slight decrease, while VFID_{ResNeXt} slightly increases, attributed to minor variations due to training uncertainty. As λ_{agn} increases, both quantitative metrics improve, indicating that the model becomes more resilient to the impact of the agnostic loss, successfully generating detailed features like accurate sleeve shapes. As shown in Fig. 5(c), compared with Fig. 5(b), the model overcomes challenging occlusions from the large agnostic mask in the initial frames, producing the expected short-sleeved dress. However, temporal consistency across the video remains suboptimal, as the short sleeves gradually "extend" into long sleeves in subsequent frames.

Finally, C&T and the setting with $\lambda_{agn} = 0.5$ improve VFID_{I3D} and VFID_{ResNeXt} decrease significantly by 2.072 and 0.0597, respectively, indicating enhanced stability. Visual results in Fig. 3 further confirm improved frame-to-frame continuity and greater garment consistency across the sequence, demonstrating the effectiveness of the combined C&T and agnostic mask-guided loss.

5. Conclusion

We propose RealVVT, a novel framework for generating accurate virtual try-on videos with both spatial and temporal consistency. Built on stable video diffusion, it integrates key innovations, including the Clothing & Temporal Consistency Attention mechanism, Agnostic Mask-Guided Loss, and Pose-guided Long VVT. Experimental results demonstrate that RealVVT produces high-quality virtual try-on videos with exceptional temporal coherence and garment consistency, while also generating high-resolution, photorealistic images suitable for virtual try-on applications. These advancements hold significant potential for enhancing realism and user engagement in e-commerce platforms.

References

- [1] A. Blattmann, T. Dockhorn, S. Kulal, D. Mendelevitch, M. Kilian, D. Lorenz, Y. Levi, Z. English, V. Voleti, A. Letts *et al.*, “Stable video diffusion: Scaling latent video diffusion models to large datasets,” *arXiv preprint arXiv:2311.15127*, 2023. [2](#), [3](#)
- [2] T. Karras, M. Aittala, T. Aila, and S. Laine, “Elucidating the design space of diffusion-based generative models,” *Advances in neural information processing systems*, vol. 35, pp. 26 565–26 577, 2022. [3](#)
- [3] D. P. Kingma, “Auto-encoding variational bayes,” *arXiv preprint arXiv:1312.6114*, 2013. [3](#)
- [4] S. Bai, H. Zhou, Z. Li, C. Zhou, and H. Yang, “Single stage virtual try-on via deformable attention flows,” in *European Conference on Computer Vision*. Springer, 2022, pp. 409–425. [3](#), [6](#)
- [5] R. Khirodkar, T. Bagautdinov, J. Martinez, S. Zhaoen, A. James, P. Selednik, S. Anderson, and S. Saito, “Sapiens: Foundation for human vision models,” in *European Conference on Computer Vision*. Springer, 2025, pp. 206–228. [6](#), [1](#)
- [6] L. Hu, “Animate anyone: Consistent and controllable image-to-video synthesis for character animation,” in *Proceedings of the IEEE/CVF Conference on Computer Vision and Pattern Recognition*, 2024, pp. 8153–8163. [2](#), [4](#)
- [7] D. Morelli, M. Fincato, M. Cornia, F. Landi, F. Cesari, and R. Cucchiara, “Dress code: High-resolution multi-category virtual try-on,” in *Proceedings of the IEEE/CVF conference on computer vision and pattern recognition*, 2022, pp. 2231–2235. [6](#)
- [8] S. Yang, Y. Zhou, Z. Liu, and C. C. Loy, “Rerender a video: Zero-shot text-guided video-to-video translation,” in *SIGGRAPH Asia 2023 Conference Papers*, 2023, pp. 1–11. [6](#)
- [9] P. Dhariwal and A. Nichol, “Diffusion models beat gans on image synthesis,” *Advances in neural information processing systems*, vol. 34, pp. 8780–8794, 2021. [3](#)
- [10] Y. Guo, C. Yang, A. Rao, Z. Liang, Y. Wang, Y. Qiao, M. Agrawala, D. Lin, and B. Dai, “Animatediff: Animate your personalized text-to-image diffusion models without specific tuning,” *arXiv preprint arXiv:2307.04725*, 2023. [3](#)
- [11] X. Ma, Y. Wang, G. Jia, X. Chen, Z. Liu, Y.-F. Li, C. Chen, and Y. Qiao, “Latte: Latent diffusion transformer for video generation,” *arXiv preprint arXiv:2401.03048*, 2024. [3](#)
- [12] R. Rombach, A. Blattmann, D. Lorenz, P. Esser, and B. Ommer, “High-resolution image synthesis with latent diffusion models,” in *Proceedings of the IEEE/CVF conference on computer vision and pattern recognition*, 2022, pp. 10 684–10 695. [3](#)
- [13] J. Zheng, F. Zhao, Y. Xu, X. Dong, and X. Liang, “Viton-dit: Learning in-the-wild video try-on from human dance videos via diffusion transformers,” *arXiv preprint arXiv:2405.18326*, 2024. [2](#), [3](#), [7](#)
- [14] Z. Xu, M. Chen, Z. Wang, L. Xing, Z. Zhai, N. Sang, J. Lan, S. Xiao, and C. Gao, “Tunnel try-on: Excavating spatial-temporal tunnels for high-quality virtual try-on in videos,” in *Proceedings of the 32nd ACM International Conference on Multimedia*, 2024, pp. 3199–3208. [2](#), [3](#), [7](#)
- [15] J. Jiang, T. Wang, H. Yan, and J. Liu, “Clothformer: Taming video virtual try-on in all module,” in *Proceedings of the IEEE/CVF Conference on Computer Vision and Pattern Recognition*, 2022, pp. 10 799–10 808. [2](#), [3](#), [7](#)
- [16] Y. Choi, S. Kwak, K. Lee, H. Choi, and J. Shin, “Improving diffusion models for authentic virtual try-on in the wild,” in *European Conference on Computer Vision*, 2024, pp. 206–235. [1](#)
- [17] J. Kim, G. Gu, M. Park, S. Park, and J. Choo, “Stableviton: Learning semantic correspondence with latent diffusion model for virtual try-on,” in *Proceedings of the IEEE/CVF Conference on Computer Vision and Pattern Recognition*, 2024, pp. 8176–8185. [7](#), [1](#), [3](#), [4](#)
- [18] J. Li, Y. Xu, T. Lv, L. Cui, C. Zhang, and F. Wei, “Dit: Self-supervised pre-training for document image transformer,” in *Proceedings of the 30th ACM International Conference on Multimedia*, 2022, pp. 3530–3539. [3](#)
- [19] A. Dosovitskiy, P. Fischer, E. Ilg, P. Hausser, C. Hazirbas, V. Golkov, P. Van Der Smagt, D. Cremers, and T. Brox, “Flownet: Learning optical flow with convolutional networks,” in *Proceedings of the IEEE international conference on computer vision*, 2015, pp. 2758–2766. [3](#)
- [20] G. Kuppa, A. Jong, X. Liu, Z. Liu, and T.-S. Moh, “Shineon: Illuminating design choices for practical video-based virtual clothing try-on,” in *Proceedings of the IEEE/CVF Winter Conference on Applications of Computer Vision*, 2021, pp. 191–200. [3](#)
- [21] X. Zhong, Z. Wu, T. Tan, G. Lin, and Q. Wu, “Mv-ton: Memory-based video virtual try-on network,” in *Proceedings of the 29th ACM International Conference on Multimedia*, 2021, pp. 908–916. [2](#)
- [22] H. Dong, X. Liang, X. Shen, B. Wu, B.-C. Chen, and J. Yin, “Fw-gan: Flow-navigated warping gan for video virtual try-on,” in *Proceedings of the IEEE/CVF international conference on computer vision*, 2019, pp. 1161–1170. [2](#), [3](#)
- [23] S. Chen, M. Xu, J. Ren, Y. Cong, S. He, Y. Xie, A. Sinha, P. Luo, T. Xiang, and J.-M. Perez-Rua, “Gentron: Diffusion transformers for image and video generation,” in *Proceedings of the IEEE/CVF Conference on Computer Vision and Pattern Recognition*, 2024, pp. 6441–6451. [3](#)
- [24] J. Jiang, G. Hong, L. Zhou, E. Ma, H. Hu, X. Zhou, J. Xiang, F. Liu, K. Yu, H. Sun *et al.*, “Dive: Dit-based video generation with enhanced control,” *arXiv preprint arXiv:2409.01595*, 2024.
- [25] Y. Liu, K. Zhang, Y. Li, Z. Yan, C. Gao, R. Chen, Z. Yuan, Y. Huang, H. Sun, J. Gao *et al.*, “Sora: A review on background, technology, limitations, and opportunities of large vision models,” *arXiv preprint arXiv:2402.17177*, 2024. [3](#)
- [26] S. Yin, C. Wu, H. Yang, J. Wang, X. Wang, M. Ni, Z. Yang, L. Li, S. Liu, F. Yang *et al.*, “Nuwa-xl: Diffusion over diffusion for extremely long video generation,” *arXiv preprint arXiv:2303.12346*, 2023. [3](#)
- [27] Z. Zhang, F. Long, Y. Pan, Z. Qiu, T. Yao, Y. Cao, and T. Mei, “Trip: Temporal residual learning with image noise prior for image-to-video diffusion models,” in *Proceedings of the IEEE/CVF Conference on Computer Vision and Pattern Recognition*, 2024, pp. 8671–8681. [3](#)

- [28] Y. He, T. Yang, Y. Zhang, Y. Shan, and Q. Chen, “Latent video diffusion models for high-fidelity long video generation,” *arXiv preprint arXiv:2211.13221*, 2022. 3
- [29] N. Kumari, B. Zhang, R. Zhang, E. Shechtman, and J.-Y. Zhu, “Multi-concept customization of text-to-image diffusion,” in *Proceedings of the IEEE/CVF Conference on Computer Vision and Pattern Recognition*, 2023, pp. 1931–1941. 3
- [30] M. Kang, R. Zhang, C. Barnes, S. Paris, S. Kwak, J. Park, E. Shechtman, J.-Y. Zhu, and T. Park, “Distilling diffusion models into conditional gans,” *arXiv preprint arXiv:2405.05967*, 2024. 3
- [31] B. Wang, H. Zheng, X. Liang, Y. Chen, L. Lin, and M. Yang, “Toward characteristic-preserving image-based virtual try-on network,” in *Proceedings of the European conference on computer vision (ECCV)*, 2018, pp. 589–604. 7
- [32] S. Lee, G. Gu, S. Park, S. Choi, and J. Choo, “High-resolution virtual try-on with misalignment and occlusion-handled conditions,” in *European Conference on Computer Vision*. Springer, 2022, pp. 204–219. 7
- [33] D. Morelli, A. Baldrati, G. Cartella, M. Cornia, M. Bertini, and R. Cucchiara, “Ladi-vton: Latent diffusion textual-inversion enhanced virtual try-on,” in *Proceedings of the 31st ACM International Conference on Multimedia*, 2023, pp. 8580–8589. 7
- [34] J. Gou, S. Sun, J. Zhang, J. Si, C. Qian, and L. Zhang, “Taming the power of diffusion models for high-quality virtual try-on with appearance flow,” in *Proceedings of the 31st ACM International Conference on Multimedia*, 2023, pp. 7599–7607. 7
- [35] S. Choi, S. Park, M. Lee, and J. Choo, “Viton-hd: High-resolution virtual try-on via misalignment-aware normalization,” in *Proceedings of the IEEE/CVF conference on computer vision and pattern recognition*, 2021, pp. 14 131–14 140. 4, 6
- [36] N. Ravi, V. Gabeur, Y.-T. Hu, R. Hu, C. Ryali, T. Ma, H. Khedr, R. Rädle, C. Rolland, L. Gustafson *et al.*, “Sam 2: Segment anything in images and videos,” *arXiv preprint arXiv:2408.00714*, 2024. 1
- [37] Z. He, P. Chen, G. Wang, G. Li, P. H. Torr, and L. Lin, “Wildvidfit: Video virtual try-on in the wild via image-based controlled diffusion models,” *arXiv preprint arXiv:2407.10625*, 2024. 2, 3, 7, 1
- [38] J. Zeng, D. Song, W. Nie, H. Tian, T. Wang, and A.-A. Liu, “Cat-dm: Controllable accelerated virtual try-on with diffusion model,” in *Proceedings of the IEEE/CVF Conference on Computer Vision and Pattern Recognition*, 2024, pp. 8372–8382. 7
- [39] A. Baldrati, D. Morelli, G. Cartella, M. Cornia, M. Bertini, and R. Cucchiara, “Multimodal garment designer: Human-centric latent diffusion models for fashion image editing,” in *Proceedings of the IEEE/CVF International Conference on Computer Vision*, 2023, pp. 23 393–23 402. 7
- [40] B. Yang, S. Gu, B. Zhang, T. Zhang, X. Chen, X. Sun, D. Chen, and F. Wen, “Paint by example: Exemplar-based image editing with diffusion models,” in *Proceedings of the IEEE/CVF Conference on Computer Vision and Pattern Recognition*, 2023, pp. 18 381–18 391. 7
- [41] Z. Fang, W. Zhai, A. Su, H. Song, K. Zhu, M. Wang, Y. Chen, Z. Liu, Y. Cao, and Z.-J. Zha, “Vivid: Video virtual try-on using diffusion models,” *arXiv preprint arXiv:2405.11794*, 2024. 2, 3, 6, 7, 1
- [42] S. Yang, Y. Zhou, Z. Liu, and C. C. Loy, “Fresco: Spatial-temporal correspondence for zero-shot video translation,” in *Proceedings of the IEEE/CVF Conference on Computer Vision and Pattern Recognition*, 2024, pp. 8703–8712. 6
- [43] Z. Huang, M. Zhang, and J. Liao, “Lvcd: reference-based lineart video colorization with diffusion models,” *ACM Transactions on Graphics (TOG)*, vol. 43, no. 6, pp. 1–11, 2024. 6
- [44] Y. Wu, A. Kirillov, F. Massa, W. Liu, A. C. Berg, and P. Dollar, “Detectron2,” 2019, accessed: 2024-12-24. [Online]. Available: <https://github.com/facebookresearch/detectron2> 6

RealVVT: Towards Photorealistic Video Virtual Try-on via Spatio-Temporal Consistency

Supplementary Material

A. More Implementation Details

The experiment is conducted on eight NVIDIA Tesla A800 GPUs. By default, we set batch size = 2 based on the input video resolution 512x384, the learning rate is set to $5e^{-5}$. We trained experiments for 3 days.

B. More Visualization on Spatial Consistency

To demonstrate the necessity of spatial consistency as discussed in this paper, we present Fig. 6, showcasing the test results of other video generation algorithms on the ViViD dataset [41]. For fairness, we include methods trained on the ViViD dataset, using both the approach and pre-trained model provided in the ViViD paper [41]. For regions masked by the agnostic mask, where the model is required to fill the missing areas, the incomplete alignment of the mask suggests that the garment should not be naively fitted to fill the mask entirely. Instead, the model should integrate both human and garment information to complete the masked regions. Visualization results show that our method achieves a more appropriate balance between leveraging human and garment information, producing significantly better results.

C. More Image Dataset Visual Result

In the experiments part, we provide quantitative comparisons with several image-based methods. In Fig. 7 and Fig. 8, we supplement this with a visual comparison between RealVVT (ours) and StableVITON [17], a concurrent work addressing the virtual try-on task that has received significant recognition. We utilize publicly available model checkpoints to generate try-on images for StableVITON. Our visual results show on the DressCode dataset, which is currently the largest high-resolution image-based try-on dataset. This dataset includes examples for lower body, upper body, and dresses, encompassing both female and male clothing changes.

While the main text focuses on visualizations using the ViViD dataset, a high-resolution video dataset that primarily features female clothing changes, DressCode allows us to demonstrate the applicability of RealVVT to male try-on tasks. Most concurrent works, such as StableVITON, IDM-VTON [16], and WildVidFit [37], emphasize upper-body clothing during training and evaluation, likely due to the greater availability of upper-body data pairs in existing datasets (*e.g.*, VITON-HD is exclusively an upper-body

dataset, and upper-body pairs dominate DressCode compared to lower-body and dress pairs).

In Fig. 8, we showcase RealVVT’s performance in handling lower-body garments. Our results highlight superior preservation of target garment color, shape, and fine details, such as trouser leg features, compared to StableVITON. To ensure fairness, we utilize the unpaired image pairs originally provided by DressCode without any manual matching. This further substantiates the robustness and generalizability of RealVVT across diverse garment types and wearer scenarios.

D. Limitations & Discussion

During the process of collecting and consolidating experimental data, we observed that existing datasets for both image-based and video-based try-on face significant issues with segmentation accuracy. These inaccuracies affect both agnostic masks and DensePose extractions, with frequent occurrences of oversized masks or masks that fail to completely cover the original clothing. Additionally, DensePose often suffers from incomplete limb detections, such as instances where legs are only partially captured despite being visible in the original video. Attempts to leverage state-of-the-art automated segmentation methods, such as SAPI-ENS [5] and SAM2 [36], yielded limited improvements and were unable to provide satisfactory segmentation performance for these datasets.

Moreover, the generation of agnostic masks and DensePose in existing video datasets often relies on image-based segmentation tools, which inherently introduce temporal inconsistencies and significant jitter across frames. While our method demonstrates robustness against temporal inconsistencies, considerable effort is still required to counteract the input data’s inherent discontinuities and instability. Addressing these challenges highlights the importance of further optimizing existing video datasets and increasing the availability of high-quality video try-on datasets, which we identify as key directions for future research.



Figure 6. The generation results for the ViViD hard cases by ViViD method and RealVVT trained on ViViD dataset at 512×384 resolution. Both test resolution is 832x624.

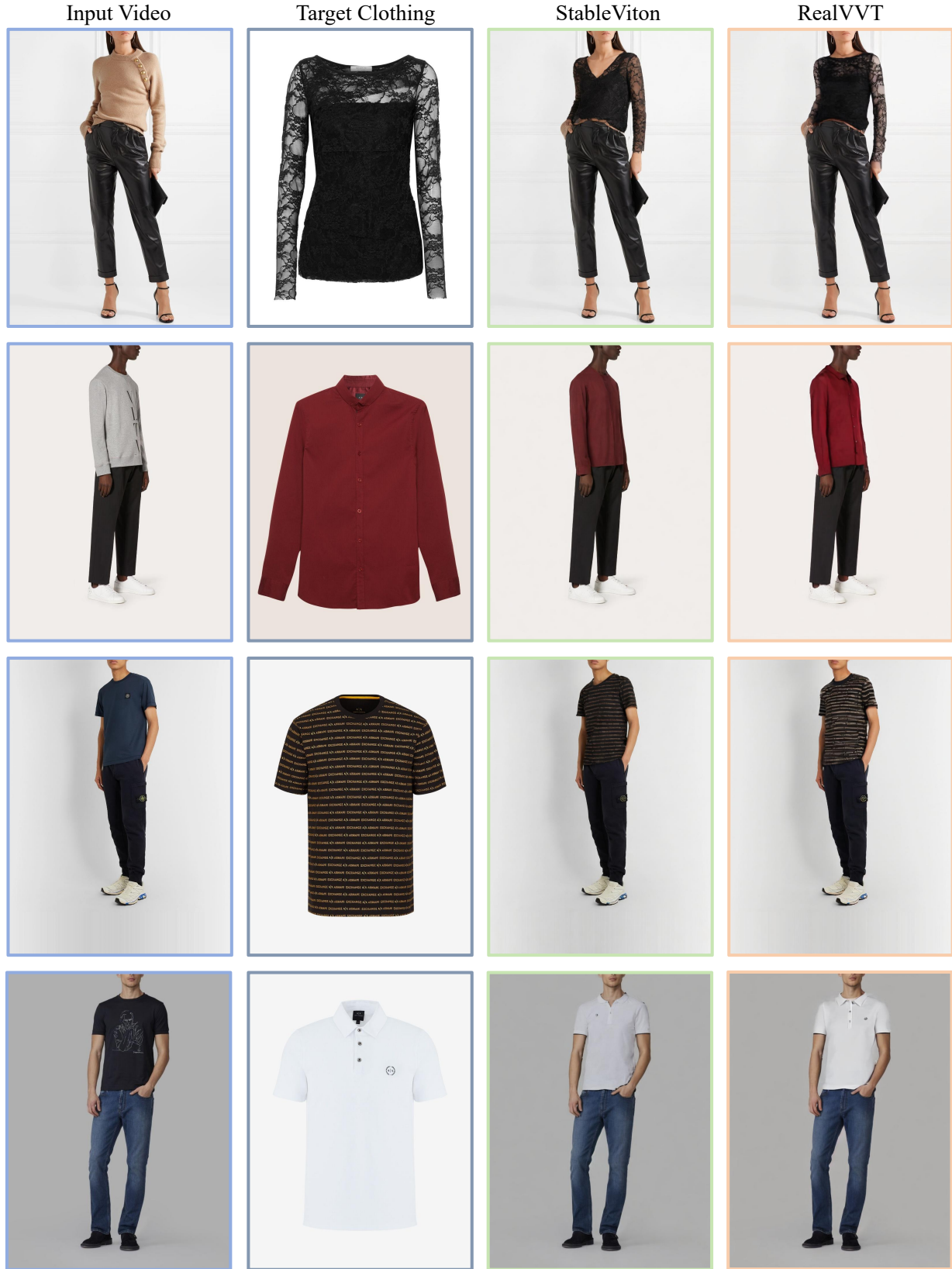


Figure 7. Comparison between StableVITON [17] and RealVVT on DressCode-Upper dataset. Comparisons demonstrate that RealVVT excels in preserving the shape and color of the target garments, particularly in maintaining finer details such as those around the collar.



Figure 8. Comparison between StableVITON [17] and RealVVT on DressCode-Lower dataset. Comparisons demonstrate that our method is better able to resist the influence of the subject’s upper body clothing and other environmental factors in the video on the newly replaced pants, allowing the generated pants to seamlessly integrate into the background and the subject while retaining their distinct characteristics.